# RESEARCH WITHIN THE IONOSPHERE

by

Robert E. Bourdeau, Space Sciences Division
NASA-Goddard Space Flight Center
Greenbelt, Maryland

As in the other space sciences, our understanding of the mechanisms which govern the characteristics of the earth's ionosphere has been enriched by the recent, golden opportunities to perform experiments on rockets and satellites which pass through the medium under study. This understanding also has been improved by the use of new and exciting ground-based experiments.

Traditionally, the ionosphere is defined as that portion of the upper atmosphere which contains a significant number of charged particles with thermal energies (tenths of an electron volt or less). Ionospheric charged particles, electrons and ions, result from ionization of the neutral constituents by ultraviolet and X-radiation from the sun and possibly by corpuscular radiation. The electrons are lost by recombination with the positive ions that are simultaneously produced. The loss rate is slow enough that the ionosphere persists throughout the night especially at the higher altitudes. Because of the high electron number density, the ionosphere classically is associated with its effects on radio cor nication processes.

In addition to the above-described production and loss-mechanisms, gravitational and electromagnetic focres contribute to ionospheric characteristics. The combination of all these factors is such that several regions with unique features are formed. This natural subdivision permits a discussion of the ionosphere to be subdivided. Specifically, as will be done here, it allows for separate discussions of the D (50-85 kilometers), the E (85-140 km) and the F (140-600 km) regions and of the upper ionosphere which extends from 600 km to several earth radii.

The D, E and that portion of the F region which lies below about 300 km were identified and named as a result of research with the classical tool of ionospheric research, the ground-based ionosonde. With this "low-frequency radar", one measures the time between transmission of a radio signal from the earth to reception of the echo reflected from the ionosphere. The electron density at the point of reflection is proportional to the square of the frequency. Therefore, when this is done as a function of frequency it is possible to obtain electron density as a function of altitude. We have learned much about the temporal and latitudinal behavior of the electron distribution in the lower ionosphere through long term world-wide use of ionosonde apparatus.

It is the purpose of this paper to summarize recent advances in our understanding of the ionosphere with e nasis on those that have come about as a result of the ability to place observatories in the medium under study. This necessarily involves relating the detailed altitude, latitude and temporal variations of all characteristics of the thermal-charged particles to gravitational and electromagnetic forces, to possible ionizing sources, and to the nature of the neutral atmosphere from which the ions and electrons are created.

## THE NEUTRAL ATMOSPHERE

The neutral atmosphere classically is divided into regions in accordance with the variation of temperature with altitude. The altitude dependence of temperature is represented for average daytime conditions[7] in Fig. 1a. Free electrons are found in significant abundance only above 50 km. Consequently, the regions of the neutral atmosphere that are of major interest to the ionosphericist are the mesosphere, which lies between the temperature maximum at 50 km and the minimum near 85 km, and the thermosphere (above 85 km).

Mesospheric temperatures have been deduced principally from rocket-borne pressure gages and by sound-velocity experiments using rocket-borne grenades. These data show that the mesosphere exhibits large latitudinal and seasonal variations.[1] The large increase of temperature in the lower thermosphere is due principally to the absorption of solar ultraviolet radiation. Heat conduction keeps the temperature nearly constant above 200 km[2]. Thermospheric temperatures have been deduced mainly from atmospheric density measured by use of gages flown on rockets[3] and satellites[4,5] and indirectly by studying satellite orbital decay[6].

From the standpoint of theories of formation of the ionosphere, the most important parameter of the neutral atmosphere is its composition. An average percentage distribution of the major constituents is presented[7] as a function of altitude in Fig. 1b. Below 100 km, mixing controls the relative abundance of the neutral constituents and consequently molecular oxygen and nitrogen predominate. Above this altitude, dissociation of atomic oxygen takes place as a result of the absorption of ultraviolet radiation by $O_2$. At the higher altitude mixing becomes unimportant and the constituents are in diffusive equilibrium, each component being distributed independently of the others. The distribution of the constituents can be calculated theoretically from the hydrostatic equation using an assumed altitude for diffusive separation and assumed atmospheric temperatures.

In Fig. 1b, it is shown that the molecular constituents diminish in importance with increasing altitude so that atomic oxygen dominates the atmosphere at 500 km. Above 500 km, the lighter gases become important. Up until an analysis of atmospheric drag on the ECHO I satellite, it was believed that there is a transition directly from an oxygen to a hydrogen atmosphere. However, this analysis[8] first suggested the existence of an intervening helium layer. The importance of neutral helium at the higher altitudes was first confirmed[5] by mass spectroscopy on the Explorer 17 satellite, some time after ionized helium had been detected from rocket[9] and satellite[10] experiments. The thickness and altitude of the helium region should be a strong function of atmospheric temperature[11]. This is reflected in the graphs (Fig. 2a) of mean molecular weight as a function of altitude for the diurnal and solar cycle extremes[12]. The region is believed to be diminishingly thin, for example, at night during the year of minimum solar activity.

The structural behavior of the atmosphere shown in Figs. 1b and 2a has been inferred principally from total density measurements using rocket-borne gages and analyses of satellite drag. Early rocket-borne mass spectrometers[13] qualitatively established that diffusive equilibrium controls the composition at the higher altitudes. However, with the early experiments was associated a high probability of errors due to surface recombination within the instruments. Consequently, it has been only in the last year that quantitatively significant measurements of the $O/O_2$ and $O/N_2$ ratios were obtained by direct sampling.[5,14,15]

Satellite drag observations show that the temperature and density of the isothermal region of the thermosphere varies considerably with time of day and with the 11-year solar cycle (Figs. 2b and 2c). The five curves[12] in Figs. 2b and 2c are for different levels of solar activity, an index of which is the 10.7 cm flux (S) measured at the earth's surface. Values for S range from 70 at sunspot minimum to 250 x $10^{-22}$ w $m^{-2}$ $(cps)^{-1}$ during the year of maximum solar activity.

THE NORMAL D REGION

The D region, which occupies approximately the same altitude interval as the mesosphere (50-85 km), is the lowest region where a significant number of free electrons a found. Here, the relatively dense atmosphere results in a high frequency of collisions between the electrons and the neutral constituents. Consequently, there is a high probability that electromagnetic energy which has been transferred to the electrons will be lost irretrievably in these collisions. Thus, the D region acts as an absorber of radio waves and from this standpoint is the most important ionospheric subdivision. Yet it is the least studied experimentally, primarily for two reasons: (a) the difficulty of devising experiments which are valid in such a weakly ionized medium and (b) the trend on the part of most ionosphericists to perform the more esoteric satellite experiments in the upper ionosphere.

In this section, we shall discuss only the "normal" D region constraining the conditions geographically to mid-latitudes and temporally to times free of solar flare effects. It wasn't until quite recently that even a preliminary model for the altitude distribution of electrons in the normal D region has evolved, despite the fact that the region is accessible with relatively inexpensive rockets.

The normal D region abundance is too low to permit study by use of the conventional ground-based ionosondes. However, break-throughs have been accomplished as a result of the development of more complex ground-based radio propagation experiments.[16,17] However, one common denominator of ground-based methods is that the altitude dependence of electron density ($N_e$) is extracted from the data only by assuming an electron collision frequency ($\nu$) profile since both $N_e$ and $\nu$ simultaneously affect the measured radio propagation phenomena. On the other hand a collaborative effort on the part of a team of Goddard and Scandinavian investigators[18,19] has resulted in novel experiments involving transmission of radio signals from the ground to rocket-borne receivers. The in-situ reception featured by these complex experiments permits unique separation of $N_e$ and $\nu$ with adequate sensitivities for the low densities found in the normal D region.

In Fig. 3, we have combined the few available rocket and ground-based observations to generate an average $N_e$ profile for the normal daytime D region (Curve A). This profile is only one of the important pieces of information required to explain how the region is formed. To complete the task requires that one relates $N_e$ to the competition between electron production and loss for each discrete altitude.

Electron production (q) can be computed from a knowledge of (a) the intensity of the ionizing radiation, (b) the density of the ionizable constituents responsive to this radiation and (c) the absorption cross-sections of the ionizable constituents. The problem of estimating q is complex because the cross-section of each individual constituent is a different function of wavelength if solar radiation is the ionizing source or of electron or proton energy for the case of corpuscular radiation.

In the D region, electron loss is believed to occur mainly through dissociative recombination of electrons with positive ions leading to an excited but neutral constituent. To estimate electron loss requires a knowledge of the recombination rates which are different for each ion species.

As a result mainly of rocket measurements of solar radiation, theoretical models[20] narrow the sources of the normal D region to three individual or combined possibilities. It generally is accepted that the lower part (50-70 km) is produced by the action of cosmic rays on the principal neutral constituents ($O_2$ and $N_2$). If so, this region should show a strong latitude dependence. There is some disagreement as to the relative roles of the remaining two sources in ionizing the upper part of the

D region. Here, one possibility involves the ionization of $O_2$ and $N_2$ by 2 - 8 Angstrom X-rays, an extremely variable source with a very low intensity (not exceeding $10^{-3}$ erg $cm^{-3}$ $sec^{-1}$ for a flareless sun). The other possibility is Lyman alpha radiation (1216A), the only ultraviolet source for which there is a favorable cross-section and which by rocket tests has been observed to penetrate into the D region. This stable but intense source measured in a few ergs $cm^{-3}sec^{-1}$ acts only upon a trace constituent, nitric oxide. Rocket and satellite measurements indicate that the X-ray fluxes at the extremes of the solar cycle vary by more than two orders of magnitude.[21] Therefore, the relative importance of X-rays and Lyman alpha radiation to the formation of the normal D region may depend on position in the solar cycle.

There have been few spaceflight input-output experiments where the ionization source and the ionization characteristics have been simultaneously measured. According to some observers[18] who measured $N_e$ on a rocket simultaneously with Lyman alpha flux, X-radiation can be ruled out as a significant source of the normal D region at least for the minimum of the solar cycle. To be certain of the relative importance of these two sources at all times, we desperately need laboratory investigations which can resolve existing uncertainties in our knowledge of the absorption cross-sections and recombination rates.

An important tool in ionospheric research is the ion spectrometer, a very difficult experiment to carry out in the D region - so difficult that it has been carried out only once[22] and this during the last year. Other than possible contaminants borne aloft by the rocket, the major ionic constituent observed below 83 km was $NO^+$. This observation supports the Lyman alpha hypothesis but does not rule out, a priori, ionization by X-radiation because of the possibility of ion-molecule interaction.[23] For example, $O_2^+$ produced directly by X-rays can react with an

$N_2$ molecule to form an $NO^+$ ion and an NO molecule. Thus, until the various reaction rates are better known, the ion spectrometer observation does not permit a choice between the Lyman alpha or the X-ray hypothesis.

SPECIAL D REGION EVENTS

There are many phenomena which can enhance the D region electron abundance by up to more than two orders of magnitude with associated electromagnetic wave attenuation strong enough to produce radio blackouts. Simultaneously with the appearance of a solar flare, increased absorption is observed in the D region on the sunlit side of the earth for periods lasting up to approximately one hour. The causative mechanisms for these sudden ionospheric disturbances (S.I.D.) were not established until investigators accurately timed rocket launchings during the course of a flare and observed enhanced X-ray activity penetrating as low as 30 km.[24] The dominant role of solar X-rays in the production of S.I.D.'s has been confirmed by correlating visible flares with satellite observations of enhanced X-ray fluxes and with increased radio absorption.[21] An order of magnitude increase in D region ionization during an S.I.D. has been measured with ground-based techniques[16] (Curve B of Fig. 3) and estimated theoretically.[20]

At high latitudes, enhanced radio absorption occurs during auroras. This is attributable to enhanced ionization resulting from direct and indirect (bremsstrahlung) effects of precipitating energetic electrons.[23] Evidence for up to a two order of magnitude increase in electron density has been obtained[19] by timing rocket flights to occur during such auroral absorption events (Curve C of Fig. 3). Another type of absorption takes place above the auroral zone and has been correlated with satellite measurements[25] of enhanced energetic proton fluxes during certain types of solar flares. There has been one rocket measurement[26] of enhanced electron densities during such polar cap absorption events

(Curve D of Fig. 3).

Increased radio absorption not associated with solar flares is often observed in the winter at middle latitudes. The causes of these events are uncertain. It has been suggested from ground-based observations[16] that these are associated with increases in electron density. However, absorption may also be associated with changes in electron collision frequency. Significant changes in $\nu$ have been correlated with measured pressure variations in the stratosphere as a result of two rocket flights during which the measured electron densities were approximately the same, thus suggesting a meteorological influence on the D region.[18]

THE E REGION

Although ground-based ionosondes have been valuable in detailing the temporal and latitudinal variations of the maximum amount of ionization found in the E and F regions, the important altitude variation of $N_e$ have come about as a result of rocket probing using both radio propagation[27,28] and plasma probe experiments.[29,30] Typical day and night $N_e$ profiles composed from such measurements are presented in Fig. 4. These show that at night the D region essentially disappears, the E region electron abundance has decreased by a hundredfold but that there is a strong persistence of the upper F region.

In addition to $N_e$ measurements, significant contributions to our understanding of the physics of the ionosphere have come about as a result of vertical cross-sections taken of the intensity of solar radiation[31] and of ionic composition.[32,33] In an important work[31], solar radiation measurements have been used together with a model neutral atmosphere to estimate the altitude dependence of (a) electron production rate for discrete portions of the X-ray and ultraviolet spectra (Fig. 5a) and (b) the rate of production of each of the ion species (Fig. 5b). We see that the ions formed at the highest rate are $O_2^+$, $N_2^+$ and $O^+$. Spectrometer observations[32] typically represented in Fig. 5c, on the other hand, show that $N_2^+$ is a minor ionic constituent despite the predicted high production rate. They also show that $NO^+$ is a dominant E region constituent even though it is not significantly produced by direct ionization. Most models[34] attribute the loss of $N_2^+$ to the combined effects of dissociative recombination with electrons and of ion-atom interchange ($N_2^+ + O \rightarrow NO^+ + N$). The existence of $NO^+$ generally is explained by ion-atom interchange involving $N_2^+$ and $O^+$.

It should be apparent that our understanding of the formation of the daytime E region has been vastly improved by the above described rocket measurements. Yet, models do disagree considerably as to even the relative importance of X-ray and ultraviolet radiation in the E region. Laboratory measurements of the various rate coefficients and additional rocket flights are needed to resolve these differences.

It wasn't until quite recently that rocket experiments were made sensitive enough for extensive studies of the nighttime E region. In Fig. 4., it is shown that $N_e$ drops below $10^3$ $cm^{-3}$ and that the region is characterized by a ledge at about 100-110 km with a valley of ionization just above. It is suggested[33] by a comparison of the results from ion spectrometers flown both during the day and for the first time at night that the maintenance of the nighttime E region is explained by slow decay through dissociative recombination without resort to a nighttime source of ionization. There also is experimental evidence from rockets for metallic ions of meteoric origin in the 100-110 km region.

A frequent anomaly of the E region is sporadic E or $E_s$ ionization. One common form of $E_s$ is a layer as thin as 0.5 km in which $N_e$ is considerably higher than the region immediately below and above, leading to reflection of radio signals at (Fig. 6) abnormally high frequencies. These layers exist at preferred altitudes[35] in the region 100-120 km. Some theories[36] explain $E_s$ ionization as the result of the combined effects of wind shear and electromagnetic forces. A correlation has been found between wind shear measured on one rocket carrying a sodium vapor release experiment and $E_s$ ionization detected on a second rocket launched almost simultaneously.[29] However, the exact relationship between $E_s$ ionization and wind shear is not clear at this time.

THE F REGION

As shown in Fig. 4, the F region contains the altitude of maximum electron density (Nm). The region is subdivided into the F1 and F2 regions because a ledge often appears in the daytime 140-200 km region.

It is important to note by comparing Figs. 4 and 5a that the altitude of maximum electron density lies well above the height of maximum electron production. These rocket results confirm previously established theoretical models which ascribe the formation of the F2 peak to charge transport mechanisms of importance comparable to photochemical processes. Specifically, these models ascribe the F2 peak formation to the competition between electron production, a height dependent decrease in electron loss rate and charge transport.

The rocket solar radiation and ion composition measurements (see Fig. 5) show that the origin of F region electrons lies principally in the production of $O^+$ ions by solar ultraviolet radiation. The dominant F region loss process is believed to be radiative recombination, a two-step process involving firstly ion-atom interchange between $O^+$ ions and $N_2$ molecules and secondly recombination of the resulting $NO^+$ ions with electrons. The slowness of this two-step process is a partial explanation for the strong persistence of the nighttime F region. The possibility that the electron loss rate decreases more rapidly with altitude than the production rate is an explanation for the experimental observations that $N_{max}$ lies above the altitude of maximum production.

Because photochemical, gravitational and electromagnetic forces all are effective, the behavior of the F region is extremely complicated. Ionosonde data taken over the last three decades show that the diurnal seasonal, solar cycle and latitude effects each produce large variations in the magnitude and altitude of $N_m$.[34] These observations have been related to time-dependent neutral atmospheres deduced from satellite drag measurements (Fig. 2) to estimate ionization, loss and diffusion rates.[37,38]

As the density of the neutral constituents decrease, the importance of photochemical processes diminish. Thus, charge transport processes become dominant and bring about the observed decrease of $N_e$ with altitude. Gravitational forces, for example, act upon the ions which, by coulomb attraction, cause the electrons to diffuse downward. In this case, the hydrostatic law can be invoked and the electron distribution is controlled by the average electron-ion temperature and the type of ion.

Before rockets and satellites penetrated the upper ionosphere, it was believed that a transition takes place from $O^+$ ions directly into the protonosphere. However, rocket[9] and satellite[10] experiments indicated that a region of helium ions separated these regions in the daytime during the middle of the solar cycle. Subsequent rocket results[39] suggest that the helium ion region disappears at night. It had been predicted[11] on the basis of the different behavior of the escape rates of hydrogen and helium that both the altitude and thickness of the helium ion region would diminish with decreasing temperature, implying a strong latitudinal and solar cycle dependency.

The role of charged particle temperatures and of ionic composition in controlling the ionosphere is illustrated by rocket measurements of charged particle density taken out to very high altitudes and presented in Fig. 7. Both a daytime and a nighttime result are illustrated. The exponential portions of both profiles provide evidence for a constant electron-ion temperature throughout the region with values of 1300° and 800°K, respectively. The change of slope in both cases is interpreted as the result of a transition from $O^+$ to lighter ions, $He^+$ being dominant above this transition for the daytime case but $H^+$ dominant at night. It is seen that the lower altitude of the transition and the relatively high importance of $H^+$ causes the surprising result that at very high altitudes the nighttime densities exceed those measured in the daytime. This may not be representative of a true diurnal variation because the two sets of data were obtained in different days.

SATELLITE STUDIES

Three different types of satellites have been used for ionospheric research each performing a different task. With Direct Measurements Satellites, one uses environmental sampling techniques to measure many ionospheric parameters, but only in the immediate vicinity of the spacecraft. The US Satellite EXPLORER VIII and the British Satellite ARIEL I each contained three major experiments for such studies. The first of these measures electron temperature by techniques similar to those developed by Langmuir in his laboratory studies of gaseous discharges. The second measures the local electron density by use of the radio-frequency impedance characteristic of a probe immersed in the medium. The third type of experiment involves the use of gridded ion traps whose principle of operation is similar to that flown on SPUTNIK III. Here, the high satellite-to-ion velocity permits the trap to act as a poor man's ion spectrometer such that both ion composition and temperature are obtained.[10]

The second category of satellite (topside sounding) involves the ingenious use of an orbiting ionosonde. As with the classical tool of ground-based ionospheric research, one measures the time between transmission of a radio signal to reception of the reflected echo. For the satellite case the reflection is from the topside of the ionosphere. By sweeping the transmitted frequency, an electron density profile for the region between the F2 maximum and the satellite altitude is measured continuously along the satellite's path. Soundings of the upper ionospheric regions have been made in a near polar orbit for two years with the Canadian Satellite ALOUETTE I, which features a swept-frequency sounder. With a swept-frequency device, one obtains good altitude resolution. The recently-launched US EXPLORER XX features fixed-frequency sounding where vertical resolution is sacrificed so as to better study horizontal irregularities.

The third type of satellite observation involves the study at the earth's surface of the arrival characteristics of radio signals transmitted from the spacecraft at frequencies which penetrate the ionosphere. Faraday rotation and doppler phenomena permit the measurement of the total electron content in a cross-section between the satellite and the receiving site. The first satellite exclusively devoted to this method is Explorer XXII, launched too recently for results to be reported here.

SATELLITE RESULTS

The major results that have come from satellite studies lie in the unique observations of the latitudinal and diurnal behavior of the regions above the F2 peak and of magnetic-field aligned irregularities.

Evidence for magnetic field control of ionospheric electron densities first came about from the use of ground-based ionosondes, which since have provided details of the bottomside characteristics of the now familiar equatorial anomaly. The morphology of this anomaly has now been obtained to altitudes of about 1000 km. In Fig. 8 are presented results[41] from the Alouette satellite of electron density as a function of magnetic dip for discrete altitudes. These results specifically are for the eastern hemisphere at 1000 local time. A general increase of electron density in the equatorial regions results from diffusion along the nearly horizontal magnetic field lines. For the particular time of day illustrated, the electron density reaches a maximum at the geomagnetic equator for altitudes above about 600 km. Below this altitude, two peaks are symmetrically located along a specific field line. The equatorial anomaly is predominantly a daytime feature of the ionosphere. The altitude above which only a single peak is formed has been termed the "dome" of the anomaly. The altitude of the dime over Singapore varies from 600 km in the early morning and evening hours to a mid-afternoon maximum of about 1000 km.[41] Similar measurements[42] suggest that the anomaly builds up later in the day along the 75th West Meridian. The diurnal behavior of the equatorial anomaly suggests that its characteristics are closely related to the competition between electron production which tends to maximize $N_e$ at the sub-solar point and diffusion along magnetic field lines which tends to produce a symmetrical $N_e$ distribution about the geomagnetic equator.

Another latitude feature of the topside ionosphere are electron density troughs which appear to be a common phenomenon at middle latitudes during ionospheric storms associated with magnetic disturbances. This is illustrated by Fig. 9, a plot of Alouette satellite measurements[42] of the frequency of reflections contours. In this illustration, applicable to 65$^o$ West Longitude, the trough is less than 5$^o$ wide and centered at 45$^o$N.

Evidence for strong magnetic control of the upper ionosphere was first inferred from electron densities measured with an rf probe on the ARIEL satellite.[43] From these observations was inferred the existence of enhanced ionization lying along three specific magnetic field shells, one of which is accounted for by the above-described equatorial anomaly. The existence of these shells of enhanced ionizations were confirmed and others discovered by the ALOUETTE satellite.[41] Some of these have been associated with the American artificial radiation belt, the heart of the inner radiation belt and near the region of maximum flux of energetic particles in the outer radiation belt. All of these observations suggest that ionization by fast particles should now be considered along with ultraviolet radiation as an ionization source for the F2 region.

A very common anomaly of the F region is the "spread F" condition, where the region shows a diffuse character generally attributed to patches of ionization having concentrations different than the immediate surroundings. An ALOUETTE satellite ionogram typical of a homogeneous ionosphere is presented in Fig. 10, the two traces corresponding to the ordinary and extraordinary modes of radio-propagation. The effectiveness of spread-F in producing multiple echoes is illustrated by comparing this ionogram with that shown in Fig. 11 which was taken during spread-F conditions. The occurrence probability of spread-F has been the subject of a thorough analysis with the ALOUETTE satellite. This analysis[44] confirms previous ground-based ionosonde studies which showed that the phenomenon is almost a permanent feature of the high latitude ionosphere, occurs only during the night near the equator and that it occurs relatively seldom at mid-latitudes.

Referring back to Fig. 9, we observe that the electron density is not a strong function of magnetic latitude between about 15 and 45$^{o}$N geographic latitude. In this region, we can expect that an important charge transport mechanism is due to gravity in which case the electron distribution is a strong function of the mean ionic mass and the average electron-ion temperature. The diurnal variation of the electron distribution in this region has been studied[45] by the use of the ALOUETTE satellite. (Fig. 12). These studies have shown the amplitude of the diurnal variation becomes smaller with increasing altitude. This would confirm a conclusion based on the rocket results shown in Fig. 7 that because of the increased relative importance of the light ionic constituents, the electron densities above 1000 km at night are higher than for a daytime condition. The diurnal variation shown in Fig. 12 have been treated in terms of ionic composition and charged particle temperature, one possible result being that for daytime at 500 km the principal ion is $O^+$ with an average electron-ion temperature of about 1500°K, while at night the lighter ionic constituents become important even at altitudes as low as 500 km.[45]

CHARGED PARTICLE TEMPERATURES IN THE UPPER IONOSPHERE

Because electron ($T_e$) and ion ($T_i$) temperatures are important to the behavior particularly of the region above 300 km, it is important to perform experimental observations of these parameters. Upon their creation, photoelectrons will possess energies in excess of the ambient electrons. They attempt to share this excess energy with the ambient electrons either by direct elastic collisions or after some of the excess energy has been lost through previous inelastic collisions with the ambient neutral particles or positive ions. As a result, there is a tendency for the ambient electron gas to be hotter than the neutral gas, at least in the daytime. It generally is accepted that at the lower altitudes where the neutral gas density is relatively high, the ion and neutral gas temperatures will be identical. At the higher altitude where the percentage ionization is becoming appreciable, there is a possibility that the ions are in better thermal contact with electrons than with the neutral particles and consequently the ion temperature can be elevated above the neutral gas temperature.[46]

Measurements made with the EXPLORER VIII satellite first indicated a strong diurnal control of ionospheric electron temperatures.[47] Later results with the ARIEL satellite[48] and with ground-based radar incoherent backscatter apparatus[49] confirmed this diurnal dependency. The ARIEL results and a comparison of radar backscatter observations at two locations[49,50] showed that there also is a strong dependency of $T_e$ upon magnetic latitude. Both the diurnal and latitudinal control of $T_e$ were subsequently confirmed[5] with the EXPLORER 17 satellite. The observations together show that the daytime ratio of $T_e$ to the neutral gas temperature can reach values up to 2 depending on latitudinal and temporal conditions.

Since newly-created electrons share their excess energy with the ambient electrons, it follows that $N_e$ and $T_e$ should be strongly coupled. The latitudinal behavior of $T_e$ for the daytime ionosphere thus can be explained in terms of magnetic field control of the electron density at least at moderate altitudes. But, it has been observed that $T_e$ increases with altitude above 600 km.[48] This would not be expected if direct effects of solar ultraviolet radiation constitute the only source of daytime charged particle heatings. The observations[48] are consistent with the hypothesis[46] of possible indirect effects of ultraviolet radiation, specifically a mechanism whereby all of the newly-created electrons do not deposit their energy in the lower F region where they are created but where some are permitted to diffuse along magnetic field lines and deposit the energy at high altitudes. Another important observation[5,48] is that the electron temperature is somewhat higher than the neutral gas temperature at night. This requires a nighttime source of particle heating having an intensity which is a small fraction[48] of the daytime ultraviolet source.

## THE UPPER IONOSPHERE

In this paper, the higher altitudes have been subdivided into the F region where $O^+$ ions dominate and the upper ionosphere where light ionic constituents are more abundent. Most observations show that on the average, the transition altitude between these two regions is about 600 km. EXPLORER VIII[51] and ARIEL[52] satellite results show that the transition is from $O^+$ to $He^+$ and then to $H^+$ as the altitude increases, at least during the middle of the solar cycle. These results also show that the thickness and altitude of the helium ion region decrease drastically from day to night. Other results show a more complicated behavior in which for nighttime conditions, and for all diurnal times during the year of minimum solar activity, helium ions are never dominant. The exact morphology of upper ionospheric composition is not yet clear.

It has been suggested[53] that the mean ionic mass is a function of the ion temperature. There already exists evidence[49] that the ion temperature in the upper ionosphere is controlled by the electron temperature which we have shown exhibits a complicated diurnal and latitudinal behavior. It is becoming clear that theoretical models of the F region, the upper ionosphere and the interdependence of these two regions need to be updated to include (a) gravitational forces into which are inserted charged particle temperatures and ionic composition that are temporally and latitudinally variable; (b) the possibility of an ionization source related to fast particles which is superimposed in the ultraviolet source and which contributes to the maintenance of the nighttime ionosphere and (c) the possibility of indirect ionization from ultraviolet radiation, specifically the effect of photoelectrons diffusing from the lower F region along magnetic field lines to deposit their energy at the higher altitudes. Thus although satellite and ground-based studies in recent years have provided a preliminary description of the charged particle parameters at high altitudes, the observations need to be extended and correlated with measurements of photoelectron and fast particle fluxes before adequate theories of formation of these regions can be formulated.

REFERENCES

1. W. Nordberg and W. G. Stroud, NASA Technical Note D-703, (1961).

2. L. Spitzer, Atmospheres of the Earth and Planets, University of Chicago Press, (1952).

3. R. Horowitz, H. E. LaGow and J. F. Guiliani, J. Geophys. Res., 64, 2287-2294, (1959).

4. G. S. Sharp, W. B. Hanson and D. D. McKibbin, J. Geophys. Res., 67, 1375, (1962).

5. N. W. Spencer, G. P. Newton, C. A. Reber, L. H. Brace and R. Horowitz, NASA Goddard Space Flight Center Report X-651-64-114, (1964).

6. L. G. Jacchia, Planetary Space Sciences, 12, 355-378, (1964).

7. F. S. Johnson, Astronautics, 8, 54, (1962).

8. M. Nicolet, J. Geophys. Res., 66, 2263, (1961).

9. W. B. Hanson, J. Geophys. Res., 67, 183-188, (1962).

10. R. E. Bourdeau, W. C. Whipple, Jr., J. L. Donley and S. J. Bauer, J. Geophys. Res., 67, 467-475, (1962).

11. S. J. Bauer, J. Atmos. Sciences, 19, 276-278, (1962).

12. I. Harris and W. Priester, J. Geophys. Res., 67, 4585-4591, (1962).

13. E. B. Meadows and J. W. Townsend, Space Research I, North-Holland Publishing Co., Amsterdam, (1960).

14. E. J. Schaefer, J. Geophys. Res., 68, 1175-1176, (1963).

15. A. O. Nier, J. H. Hoffman, C. Y. Johnson and J. C. Holmes, J. Geophys. Res., 69, 979-989, (1964).

16. J. S. Belrose and E. Cetiner, Nature, 195, 688, (1962).

17. R. E. Barrington and E. V. Thrane, J. Atmos. Terr. Phys., 24, 31, (1962).

18. A. C. Aikin, J. A. Kane and J. Troim, J. Geophys. Res., (November 1964).

19. M. Jespersen, O. Petersen, J. Rybner, B. Bjelland, O. Holt and B. Landmark, Norwegian Space Res. Comm. Rept. No. 3, (1963).

20. M. Nicolet and A. C. Aikin, J. Geophys. Res., 65, 1469, (1960).

21. H. Friedman, Astronautics, 8, 14, (1962).

22. R. S. Narcisi and A. D. Bailey, Space Research V, (to be published).

23. A. C. Aikin, International Dictionary of Geophysics, (1964).

24. T. A. Chubb, H. Friedman, R. W. Kreplin and J. E. Kupperian, J. Geophys. Res., 62, 389, (1957).

25. B. Maehlum and B. J. O'Brien, J. Geophys. Res., 67, (1961).

26. J. E. Jackson and J. A. Kane, J. Geophys. Res., 64, 1074, (1959).

27. J. C. Seddon and J. E. Jackson, Ann. de Geophys., 14, 456, (1958).

28. J. E. Jackson and S. J. Bauer, J. Geophys. Res., 66, 3055, (1961).

29. L. G. Smith, Geophys. Corp. America, Tech. Rept. 62-1-N, (1962).

30. W. B. Hanson and D. D. McKibbin, J. Geophys. Res., 66, 1667, (1961).

31. K. Watanabe and H. E. Hinteregger, J. Geophys, Res., 67, 999, (1962).

32. H. A. Taylor and H. C. Brinton, J. Geophys. Res., 66, 2587, (1961).

33. J. C. Holmes, C. Y. Johnson and J. M. Young, Space Research V, (in press).

34. T. E. Van Zandt and R. W. Knecht, Space Physics, D. P. Galley and A. Rosen, ed., John Wiley and Sons, New York, (1964).

35. J. C. Seddon, Ionospheric Sporadic E, Pergamon Press, Oxford, 909, (1962).

36. J. D. Whitehead, J. Atmos. Terr. Phys., 20, 49, (1961).

37. H. Rishbeth, J. Atmos. Terr. Phys., 26, 657, (1964).

38. J. S. Nisbet and T. P. Quinn, J. Geophys. Res., 68, 1031, (1963).

39. J. L. Donley, J. Geophys. Res., 68, 2058, (1963).

40. S. J. Bauer and J. E. Jackson, J. Geophys. Res., 67, 1675, (1962).

41. King, J. W., P. A. Smith, D. Eccles and H. Helm, Radio Research Station Report 94, Bucks, England, (1963).

42. Lockwood, G. E. K. and G. L. Nelms, J. Atmos. Terr. Phys., (1964), in press.

43. Sayers, J., P. Rothwell and J. H. Wager, Nature, 198, 230, (1963).

44. Calvert, W. and C. W. Schmid, J. Geophys. Res., 69, 1839-1852 (1964).

45. Bauer, S. J. and L. Blumle, J. Geophys. Res., 69, 3613-3618 (1964).

46. Hanson, W. B., Space Research III, 282, (1962).

47. Serbu, G. P., R. E. Bourdeau and J. L. Donley, J. Geophys. Res., 66, 4313-4319 (1961).

48. Willmore, A. P., Proceedings of the Royal Society Meeting, May 1963, in press.

49. Evans, J. V., J. Geophys. Res., 67, 4914-4920 (1962).

50. Bowles, K. L., J. Research NBS, 65D, 1-14 (1961).

51. Bourdeau, R. E. and J. L. Donley, Proceedings of Royal Society Conference May 1963, in press.

52. Boyd, R. L., Proceedings of the Royal Society Conference, May 1963, in press.

53. Bauer, S. J., J. Geophys. Res., 69, 553-555 (1964).

## FIGURE CAPTIONS

FIGURE 1. Altitude dependence of neutral gas temperature and fractional composition (Johnson, 1962).

FIGURE 2. Time-dependent model of neutral gas (a) mean molecular weight, (b) thermospheric temperature, and (c) 600 km density, Harris and Priester (1962).

FIGURE 3. D Region Electron Density Profiles.

FIGURE 4. Typical D, E and F Region Electron Density Profiles.

FIGURE 5. Comparison of ion production rates (Watanabe and Hinteregger, 1962) with rocket measurement of ionic composition (Taylor and Brinton, 1961).

FIGURE 6. Rocket detection of sporadic-E layer (Smith, 1962).

FIGURE 7. Daytime (Bauer and Jackson, 1962) and nighttime (Donley, 1963) measurements of electron density.

FIGURE 8. Contours of electron density at constant altitudes measured above Singapore at 1000 LMT (King et al, 1963).

FIGURE 9. Contours of constant plasma frequency measured with the Alouette satellite (Lockwood and Nelms, 1964).

FIGURE 10. Typical ionogram from ALOUETTE Satellite taken in the absence of spread-F.

FIGURE 11. ALOUETTE Satellite ionogram taken during the presence of spread-F.

FIGURE 12. Diurnal variation of electron density in the topside ionosphere (Bauer and Blumle, 1964).

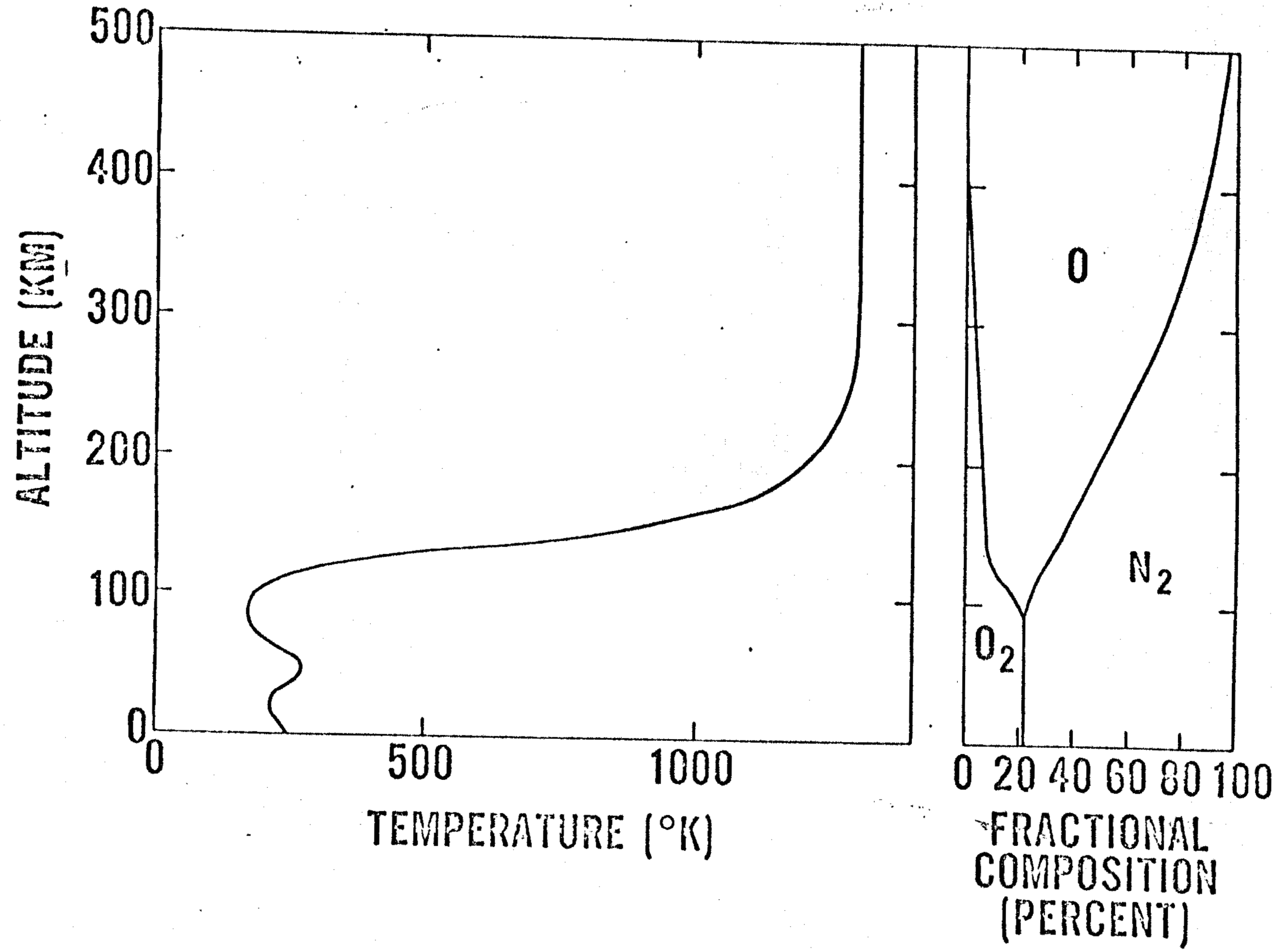

ALTITUDE (KM)
500
400
300
200
100
0
0
500
1000
TEMPERATURE (°K)
O
N2
O2
0 20 40 60 80 100
FRACTIONAL COMPOSITION (PERCENT)


1

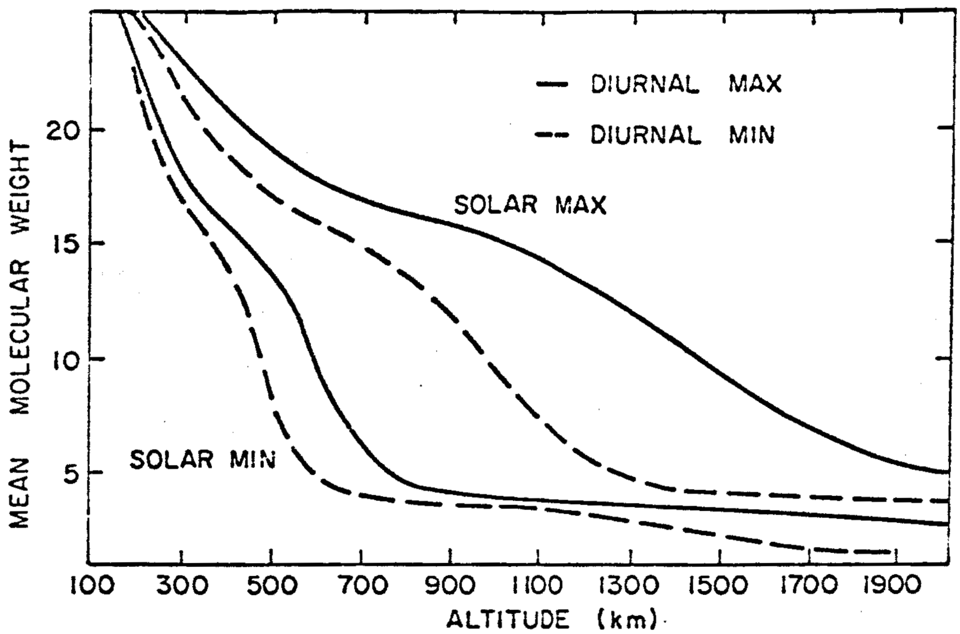
DIURNAL MAX
DIURNAL MIN
SOLAR MAX
SOLAR MIN
MEAN MOLECULAR WEIGHT
20
15
10
5
100
300
500
700
900
1100
1300
1500
1700
1900
ALTITUDE (km)

(a)

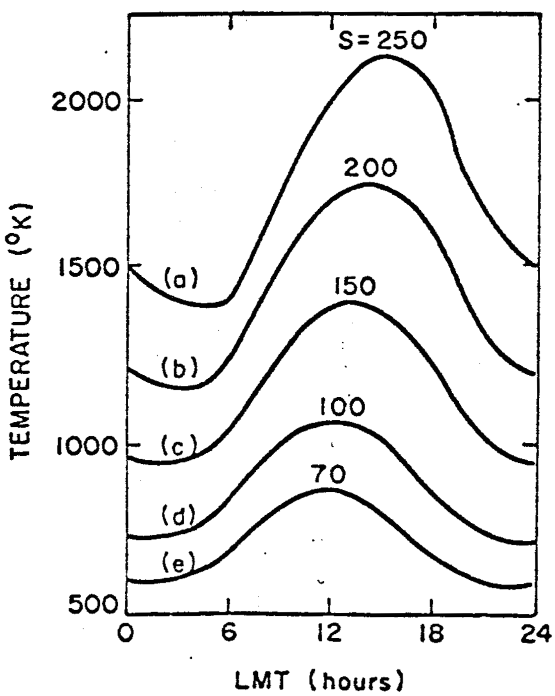
S=250
200
150
100
70
(a)
(b)
(c)
(d)
(e)
TEMPERATURE (°K)
2000
1500
1000
500
0
6
12
18
24
LMT (hours)

(b)

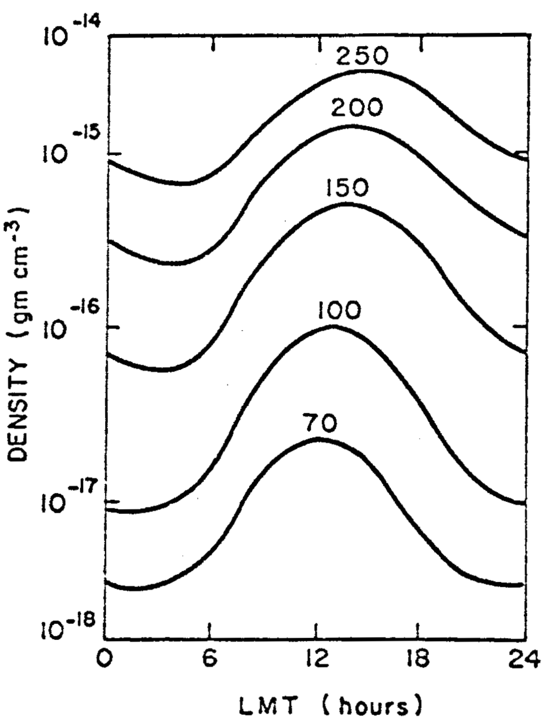
250
200
150
100
70
DENSITY (gm cm-3)
10-14
10-15
10-16
10-17
10-18
0
6
12
18
24
LMT (hours)

(c)

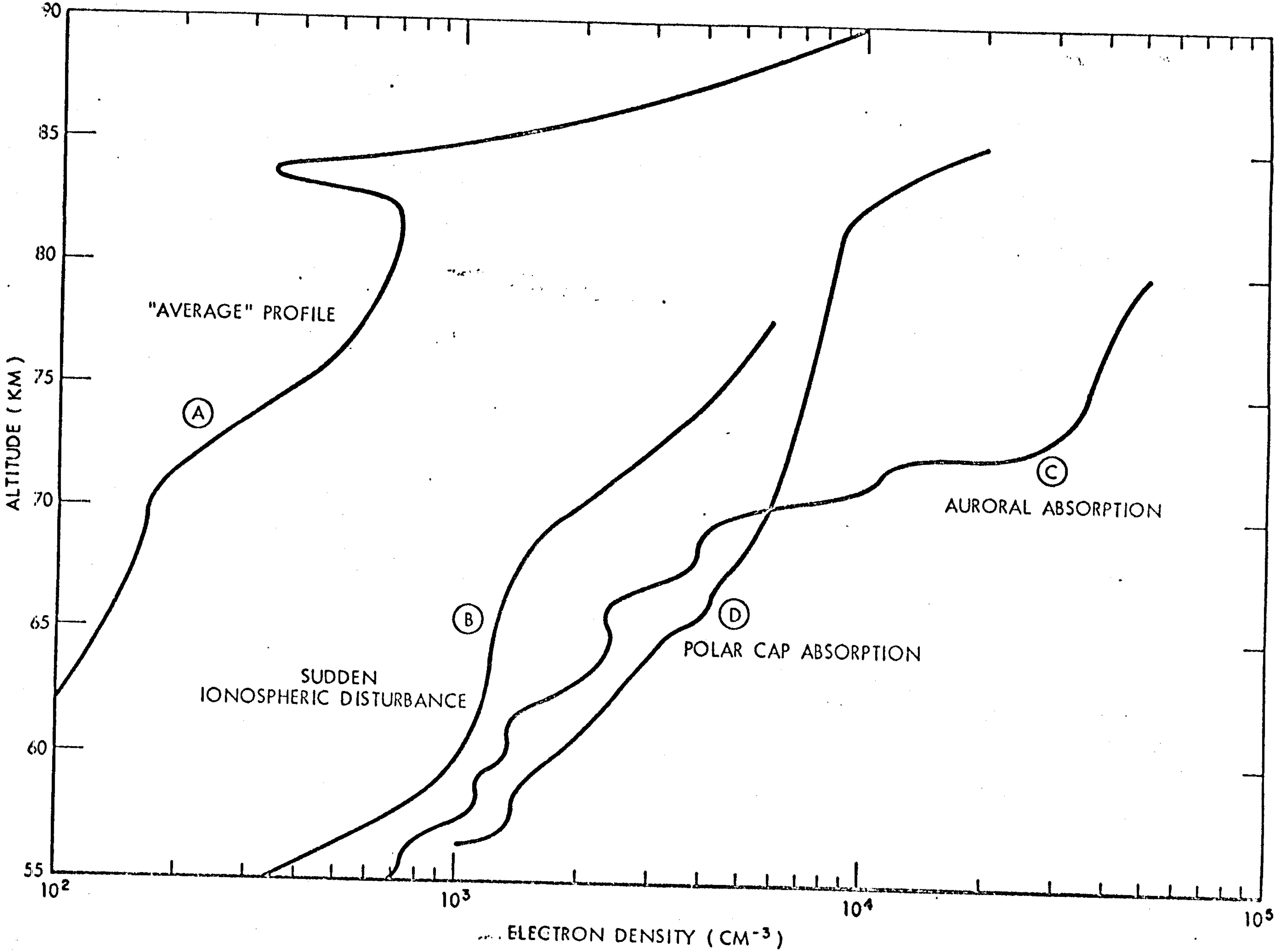

90
85
80
75
70
65
60
55
ALTITUDE ( KM )
"AVERAGE" PROFILE
A
B
SUDDEN
IONOSPHERIC DISTURBANCE
C
AURORAL ABSORPTION
D
POLAR CAP ABSORPTION
10²
10³
10⁴
10⁵
ELECTRON DENSITY ( CM⁻³ )


3

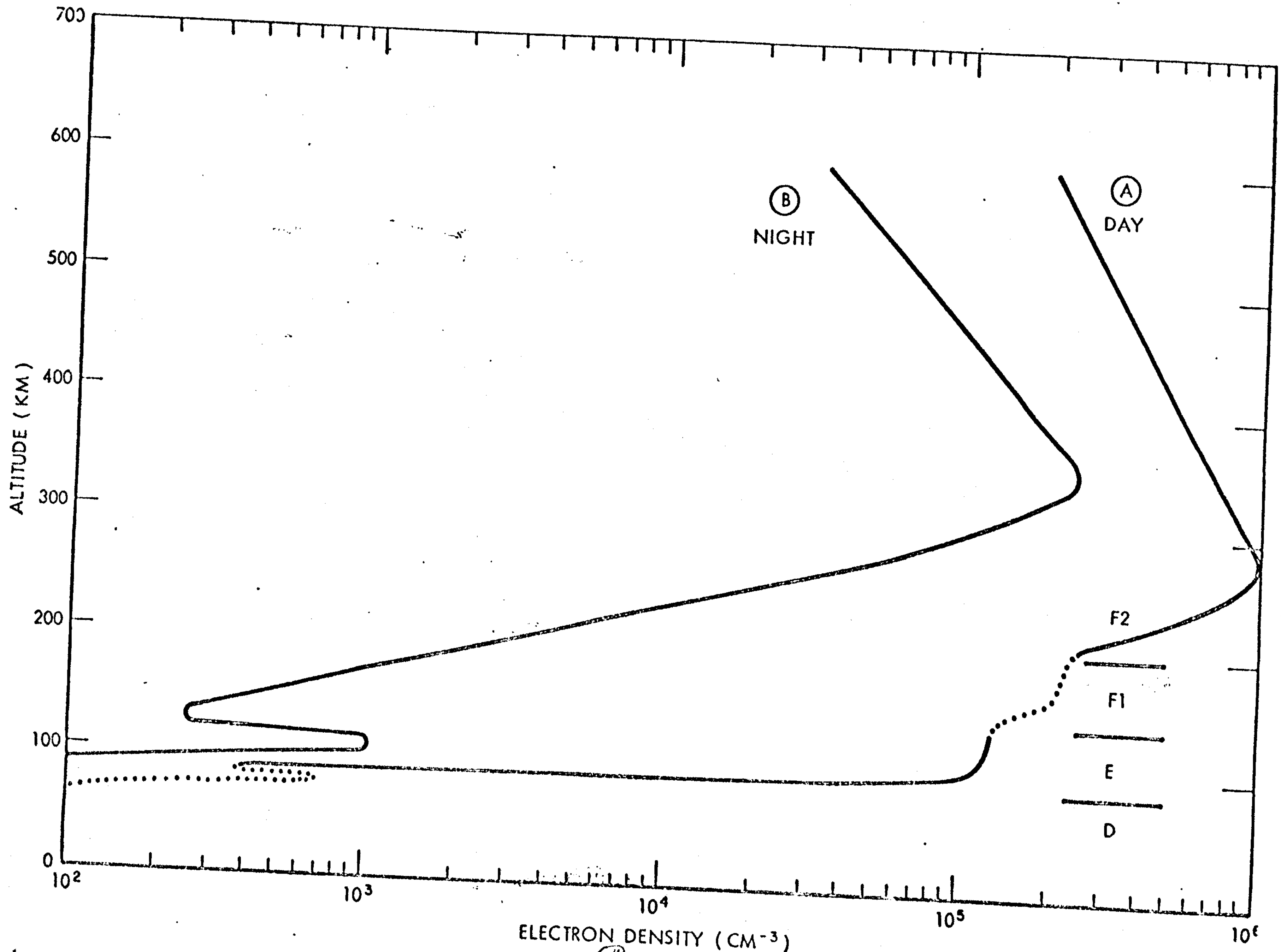

700
600
500
400
300
200
100
0
ALTITUDE ( KM )
$10^2$
$10^3$
$10^4$
$10^5$
$10^6$
ELECTRON DENSITY ( $CM^{-3}$ )
B
NIGHT
A
DAY
F2
F1
E
D


(4)

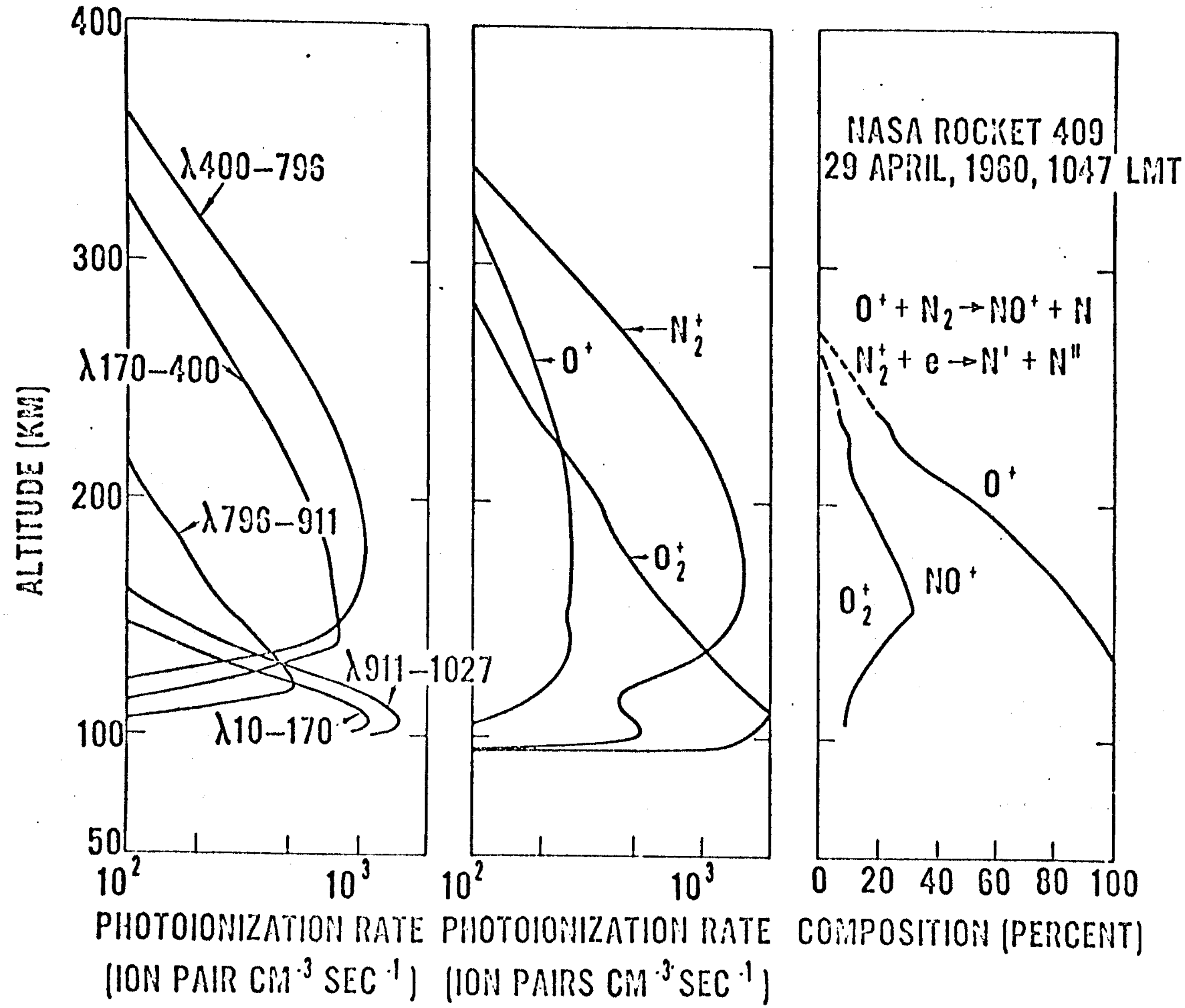

ALTITUDE (KM)
400
300
200
100
50
λ400–796
λ170–400
λ796–911
λ911–1027
λ10–170
$10^2$
$10^3$
PHOTOIONIZATION RATE
(ION PAIR $CM^{-3}$ $SEC^{-1}$)
$N_2^+$
$O^+$
$O_2^+$
PHOTOIONIZATION RATE
(ION PAIRS $CM^{-3}$ $SEC^{-1}$)
NASA ROCKET 409
29 APRIL, 1960, 1047 LMT
$O^+ + N_2 \rightarrow NO^+ + N$
$N_2^+ + e \rightarrow N' + N''$
$O^+$
$NO^+$
$O_2^+$
0 20 40 60 80 100
COMPOSITION (PERCENT)

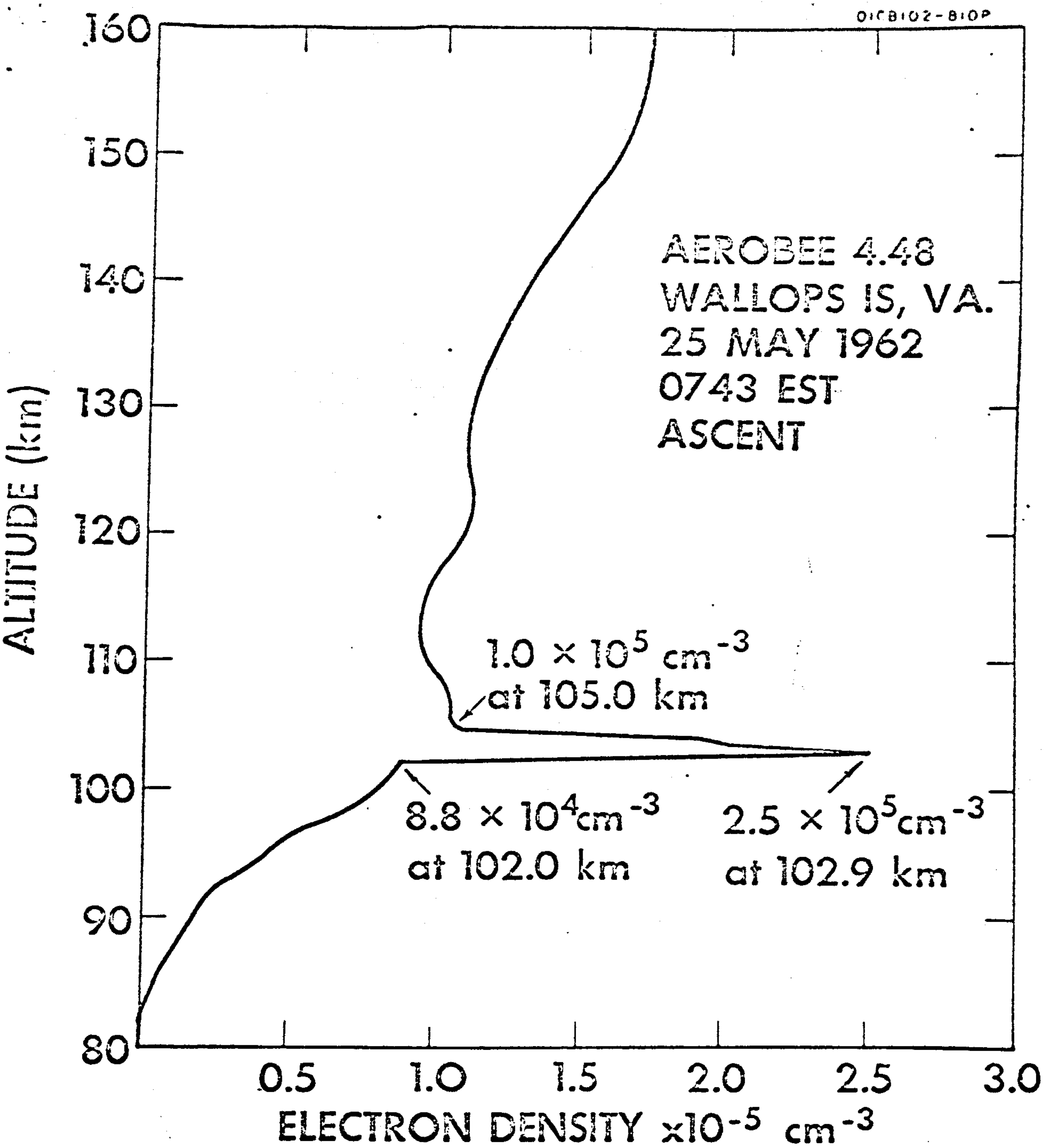
01CB102-810P
AEROBEE 4.48
WALLOPS IS, VA.
25 MAY 1962
0743 EST
ASCENT
1.0 × 10^5 cm^-3
at 105.0 km
8.8 × 10^4 cm^-3
at 102.0 km
2.5 × 10^5 cm^-3
at 102.9 km
ALTITUDE (km)
160
150
140
130
120
110
100
90
80
0.5
1.0
1.5
2.0
2.5
3.0
ELECTRON DENSITY x10^-5 cm^-3

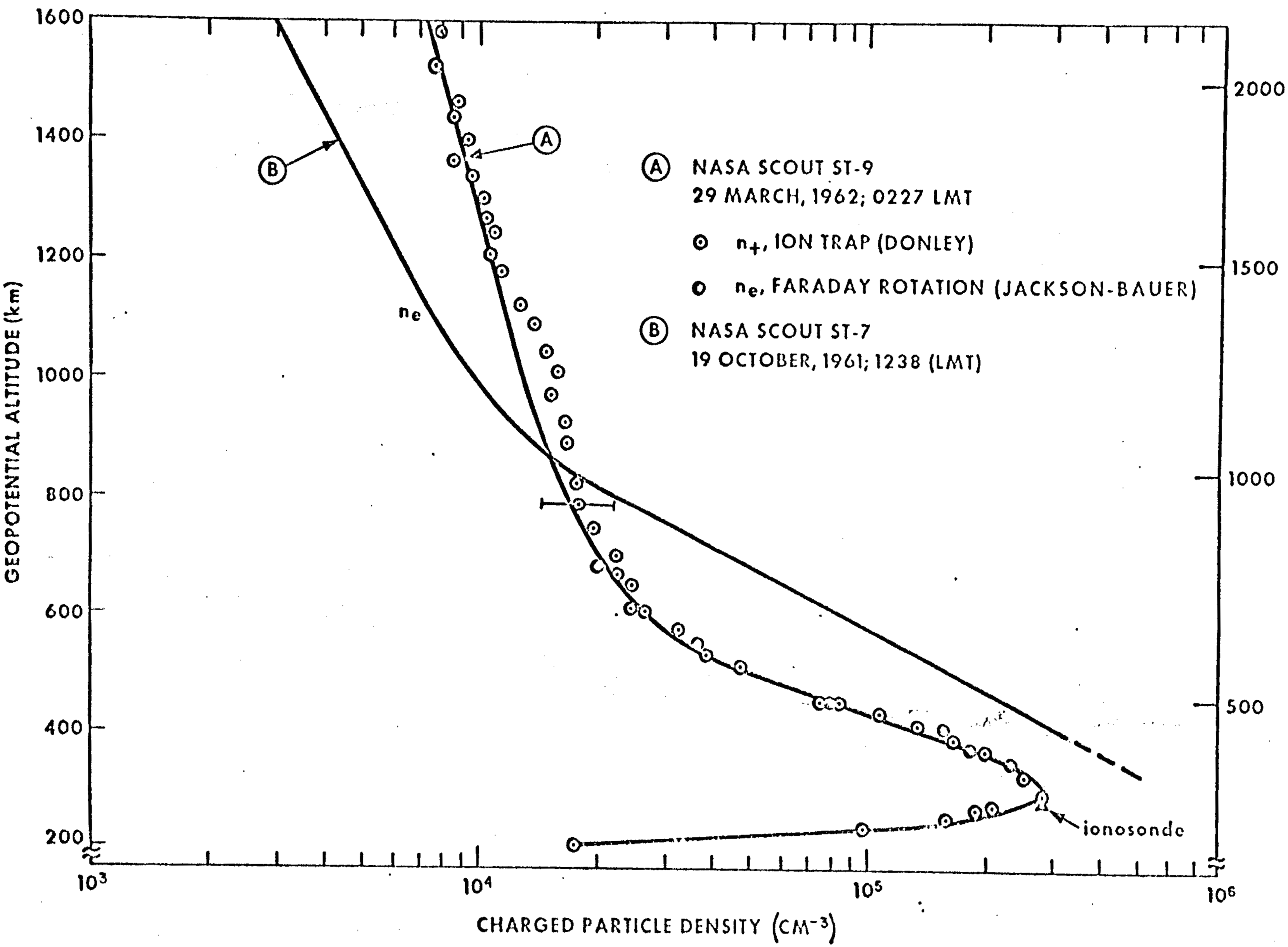

1600
1400
1200
1000
800
600
400
200
GEOPOTENTIAL ALTITUDE (km)
2000
1500
1000
500
GEOMETRIC ALTITUDE (km)
$10^3$
$10^4$
$10^5$
$10^6$
CHARGED PARTICLE DENSITY ($CM^{-3}$)
A
B
$n_e$
ionosonde
(A) NASA SCOUT ST-9
29 MARCH, 1962; 0227 LMT
$n_+$, ION TRAP (DONLEY)
$n_e$, FARADAY ROTATION (JACKSON-BAUER)
(B) NASA SCOUT ST-7
19 OCTOBER, 1961; 1238 (LMT)


(7)

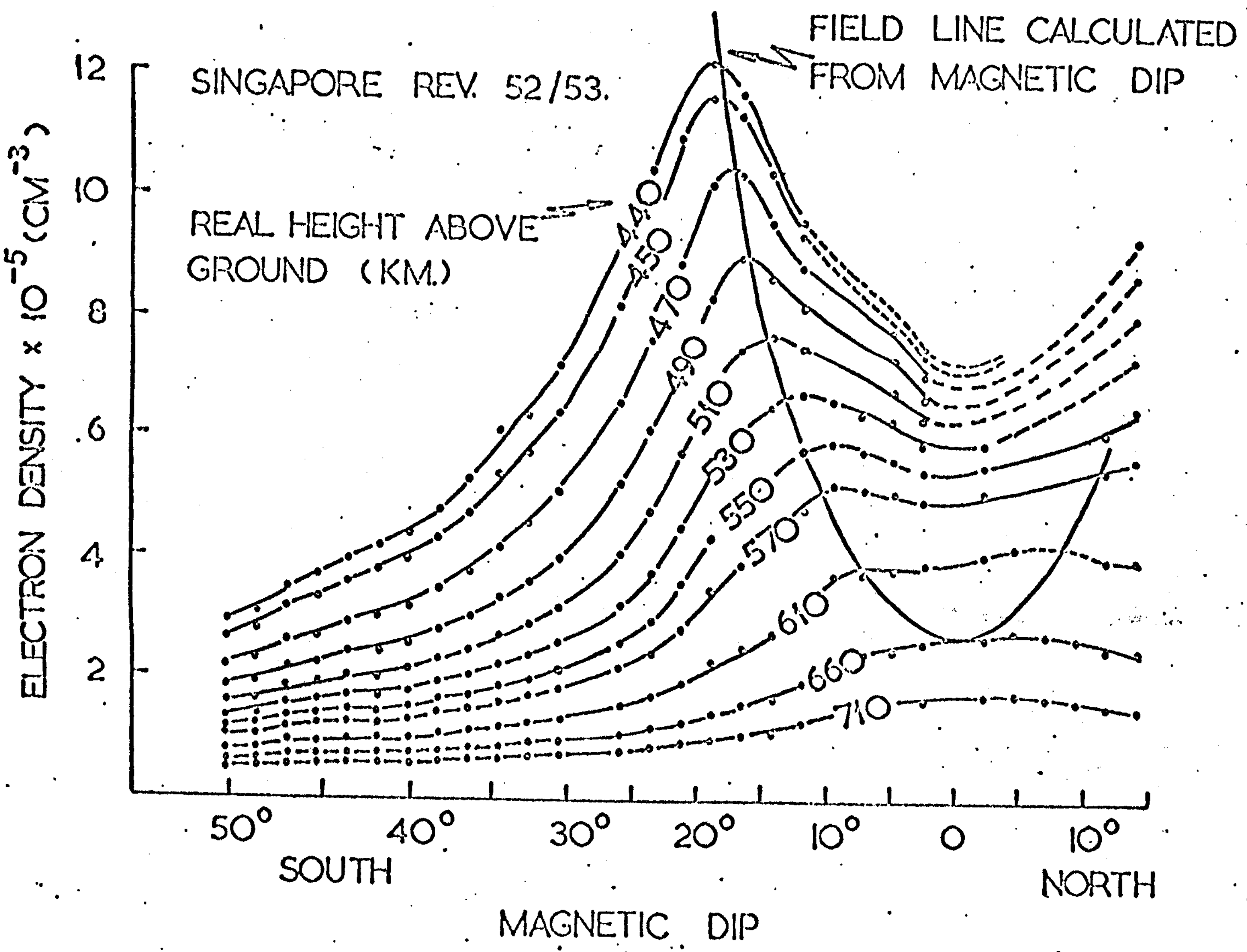

SINGAPORE REV. 52/53.
FIELD LINE CALCULATED FROM MAGNETIC DIP
REAL HEIGHT ABOVE GROUND (KM.)
440
450
470
490
510
530
550
570
610
660
710
ELECTRON DENSITY × 10^-5 (CM^-3)
12
10
8
6
4
2
50°
40°
30°
20°
10°
0
10°
SOUTH
NORTH
MAGNETIC DIP


(8)

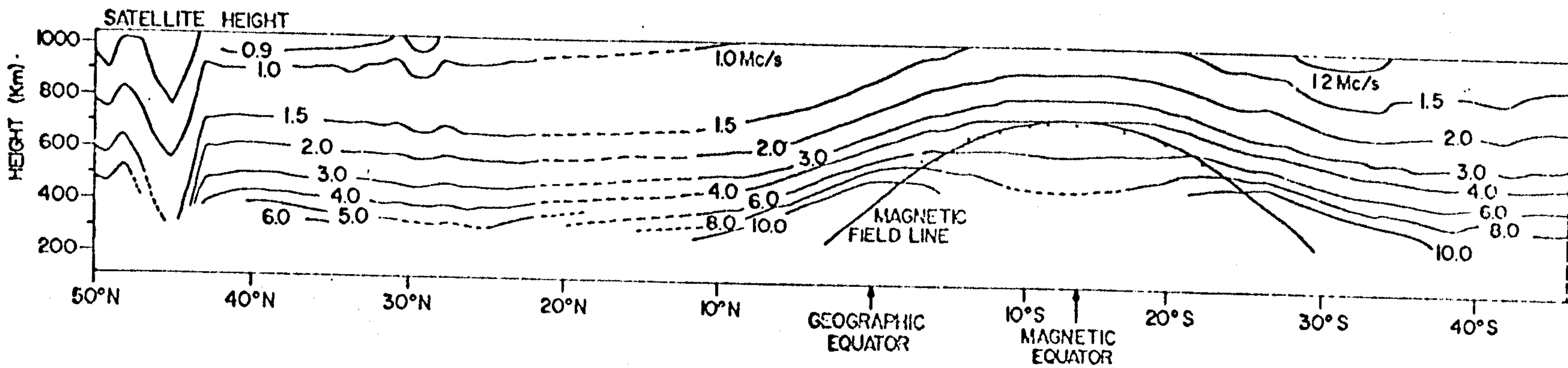


GEOGRAPHIC LATITUDE 24 OCTOBER 1962 2318 HRS. GMT.

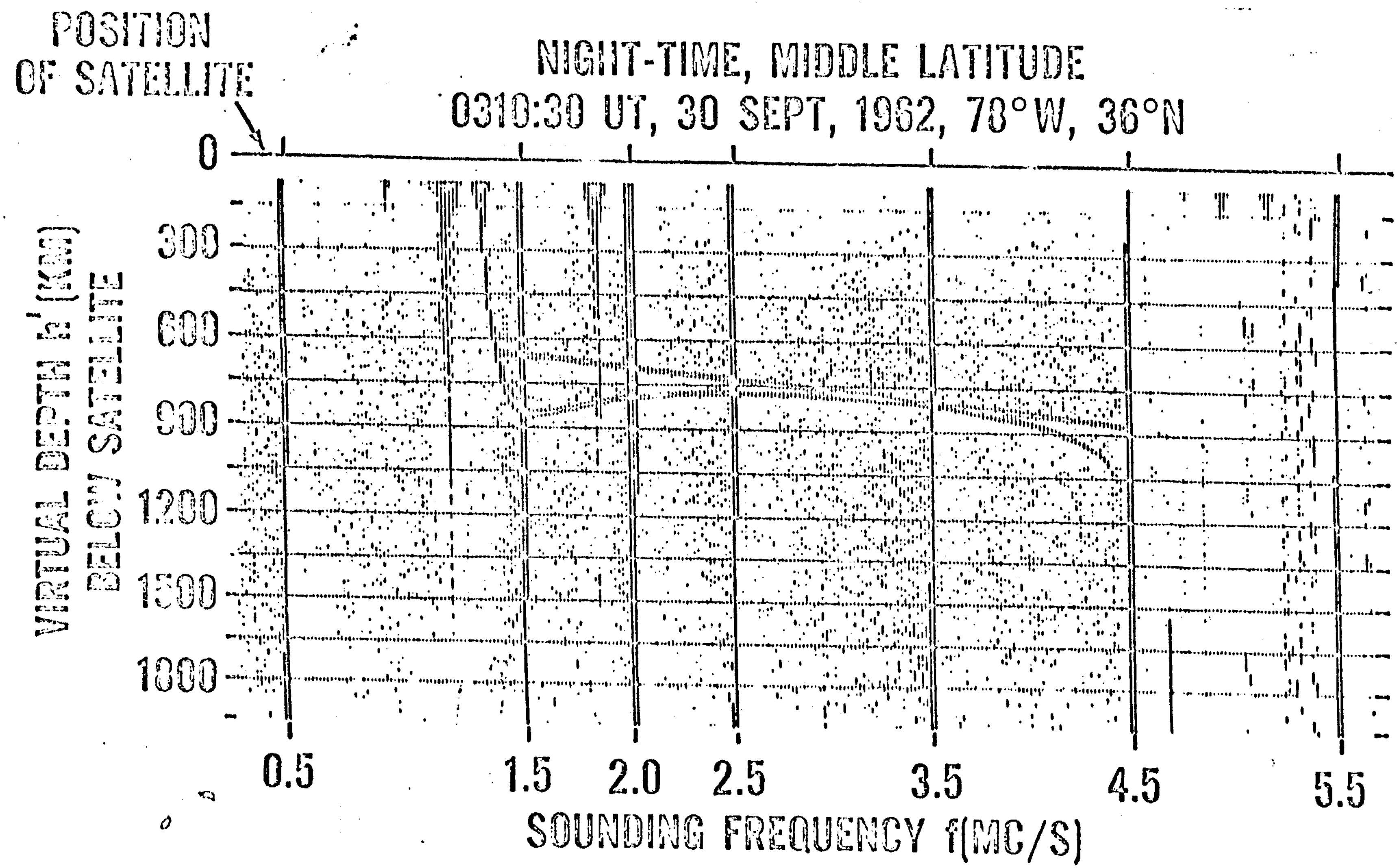

POSITION OF SATELLITE
NIGHT-TIME, MIDDLE LATITUDE
0310:30 UT, 30 SEPT, 1962, 78°W, 36°N
VIRTUAL DEPTH h' (KM) BELOW SATELLITE
0
300
600
900
1200
1500
1800
0.5
1.5
2.0
2.5
3.5
4.5
5.5
SOUNDING FREQUENCY f(MC/S)


(10)

NIGHT-TIME, HIGH LATITUDE
(23:37 EDT 1 OCT,1962 68°N 107°W)

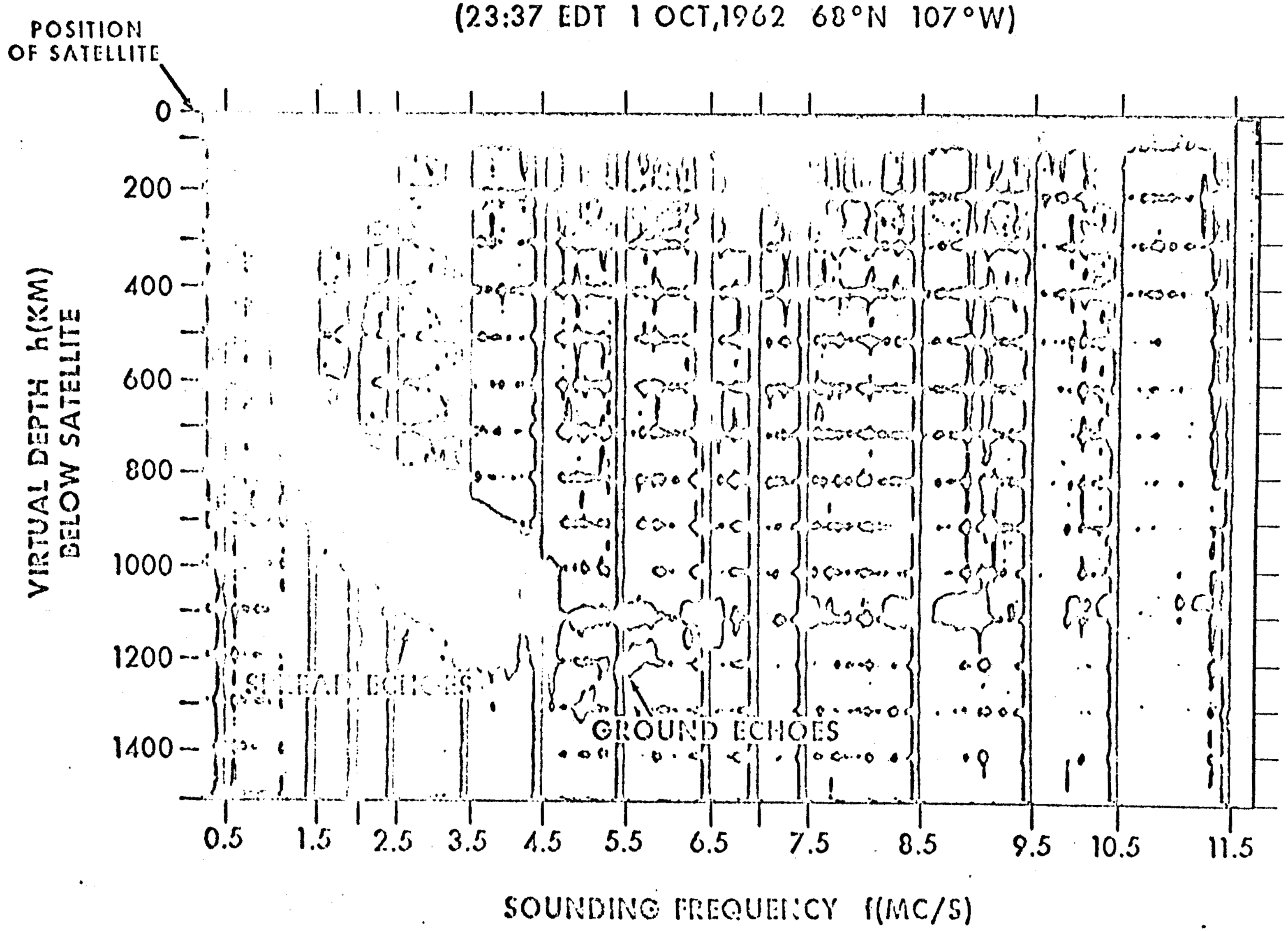

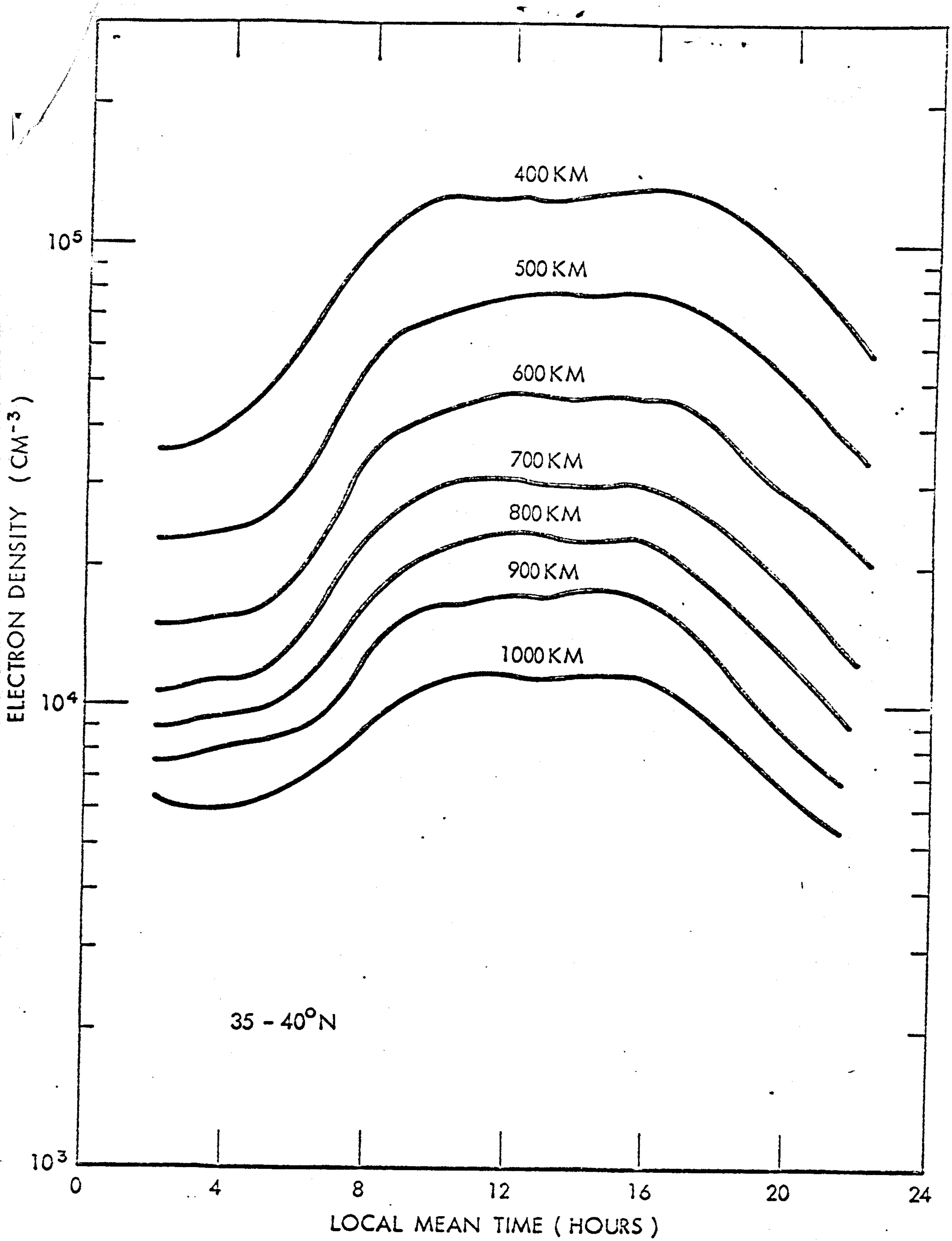

400 KM
500 KM
600 KM
700 KM
800 KM
900 KM
1000 KM
35 - 40°N
ELECTRON DENSITY (CM-3)
10^5
10^4
10^3
0
4
8
12
16
20
24
LOCAL MEAN TIME ( HOURS )